PROCEEDINGS OF SCIENCE

Reliability and fault-tolerance strategy in CADS linac and beam commissioning of CADS injector-I

Cai Meng[1]
Key Laboratory of Particle Acceleration Physics & Technology, Insititute of High Energy Physics,CAS
19B YuquanLu, Shijingshan District, Beijing, China
E-mail: mengc@ihep.ac.cn
Jianping Dai, Biao Sun, Jingyu Tang, Zhou Xue, Fang Yan
Key Laboratory of Particle Acceleration Physics & Technology, Insititute of High Energy Physics,CAS
19B YuquanLu, Shijingshan District, Beijing, China

The CADS (China Accelerator Driven Subcritical System) project is a strategic plan to solve the nuclear waste and resource problems for nuclear energy in China. The CADS driver linac is defined to deliver a CW proton beam of 15 MW in beam power. To meet the extremely high reliability and availability for high power accelerator, it is very important and imperative to perform robust design and redundancy for element failures. For robust design we give the baseline design of accelerator with reasonable and deliberate rules, meanwhile beam loss control is the most important and critical issues at the design process, so detailed error study and mismatch study have been proposed. For redundancy study the failure effects of key elements such as RF cavities and focusing elements in different locations along the linac have been studied and the schemes of compensation by the local compensation–rematch method have been proposed. Local compensation-rematch method and global compensation-rematch method have been discussed. At the last part of this paper the beam commissioning of CADS injector-I will be presented and the injector-I have got 10.67 MeV and 10.6 mA beam.

4th Workshop on ADS and thorium
31 August - 2 September 2016
University of Huddersfield, England

[1]Speaker

PoS(ADST2016)015

1. Introduction

The ADS project in China (CADS) is a strategic plan to solve the nuclear waste problem and the resource problem for nuclear power plants in China. For the CADS accelerator that is a CW proton linac with 15 MW beam power of energy 1.5 GeV and current 10 mA [1]. To save cost maybe beam energy is 1.0 GeV and current is 15 mA [2]. The CADS accelerator uses superconducting acceleration structures, except for the RFQs and is composed of two parallel injectors, a joint MEBT (Medium Energy Beam Transport) line, a main linac, and a HEBT (High Energy Beam Transport) line, which is shown in Fig.1. The RF frequencies for the main linac have been chosen as 325 MHz for the spoke cavity sections and 650 MHz for the elliptical cavity sections. However, two different designs employing different RF frequencies are pursued for the low-energy part, namely, injectors in the technical developing phase, with 325 MHz for Injector Scheme-I and 162.5 MHz for Injector Scheme-II.

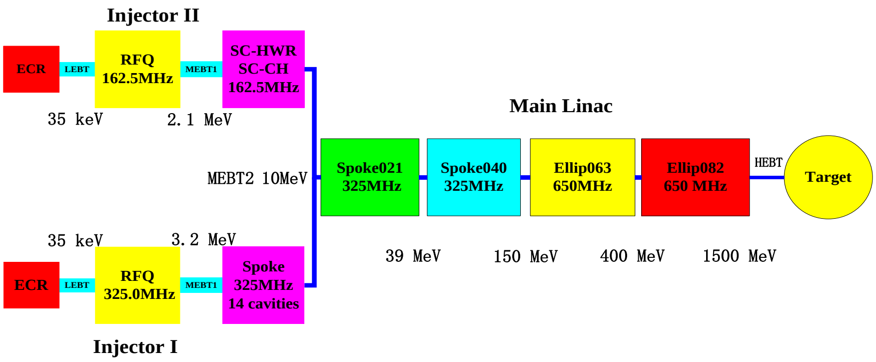

Figure 1: Layout of the CADS accelerator.

The main design specifications for the proton beam are shown in Table 1. In the last several years, more thorough and detailed beam trip requirement analyses have been performed based on transient analyses of ADS reactor system components and we adopt the common requirements which is shown in Fig.2. The beam trip requirement analyses is understudying in CADS project and new requirement for CADS will be explicit in the near further.

Table 1: Main design specifications of CADS linac

Particle	Proton	
Energy	1.5	GeV
Current	10	mA
Beam power	15	MW
RF frequency	(162.5)/325/650	MHz
Duty factor	100	%
Beam Loss	<1	W/m
	<25000	1 s<t<10 s
Beam trips/year [3]	<2500	10 s<t<5 m
	<25	t >5 m

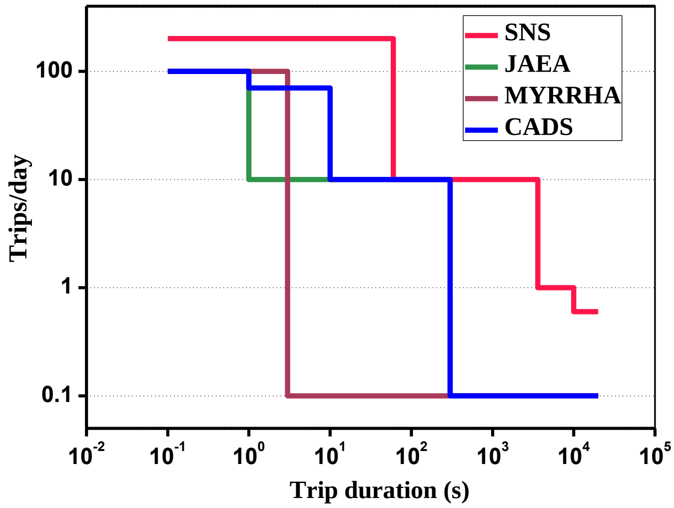

Figure 2: Beam trip comparison for different accelerator.

As shown at above part the requirement of reliability and availability is extremely high, meanwhile the beam loss rate is extremely low. To meet the requirement, it is very important and imperative to perform robust design and redundancy for element failures. The robust design will be presented in section 2 and the redundancy study will be discussed in section 3, at the last section the beam commissioning of CADS injector-I will be presented and we got very good results.

2. Robust design

2.1.1. Design rules

As mentioned before, robust design is required for ADS linacs to obtain very high reliability. According to the state-of-art performance and the prototype experience, we define some key rules for the physics design of the CADS linac.

1) Keep zero-current period phase advances are smaler than 90 degree in all planes to avoid structure and space charge driven resonances[4][5]: envelope instability or 4th order resonances. Figure 3 (left) shows the zero-current period phase advances of the CADS linac.

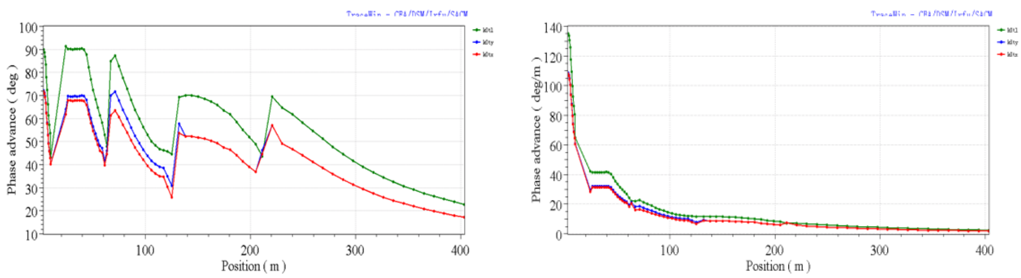

Figure 3: Zero-current period phase advance (left) and phase advacne per meter (right) of the CADS linac.

2) Keep "smooth" phase advance and provide good matching between sections in all planes to minimise emittance growth. Phase advaces per meter of the CADS linac are shown in Fig.3 (right).

3) Equipartitioning design are adopted by most accelerator designs, however equipartitioning beam is not necessary to avoid emittance exchanged, and it would be sufficient if one avoids

resonance region in the Hofmann chart [6]. In CADS linac design we keep the ratio between the longitudinal and transverse phase advance around kz/kx=1.25 to avoid emittance exchange between transverse and longitudinal planes via space charge and maximize the use of the available accelerating gradient [7], which are shown in Fig.4.

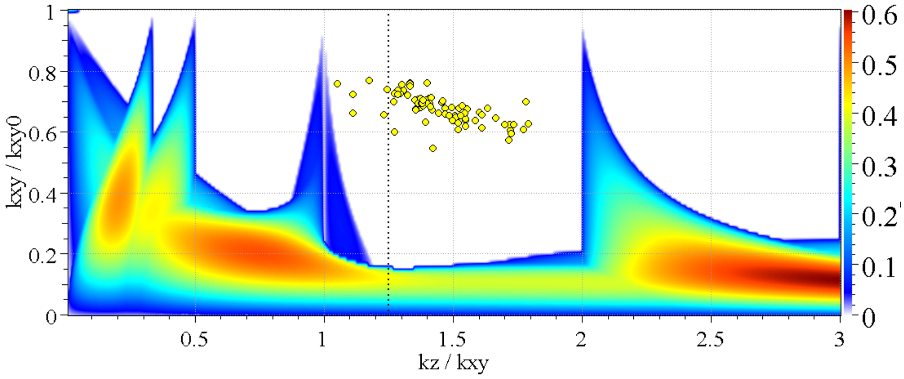

Figure 4: Hofmann chart and working point for the CADS linac.

4) Keep tune depressions are larger than 0.4 to avoid emittance growth [8]. For the CADS linac the tune depressions are larger than 0.5 and shown in Fig.5.

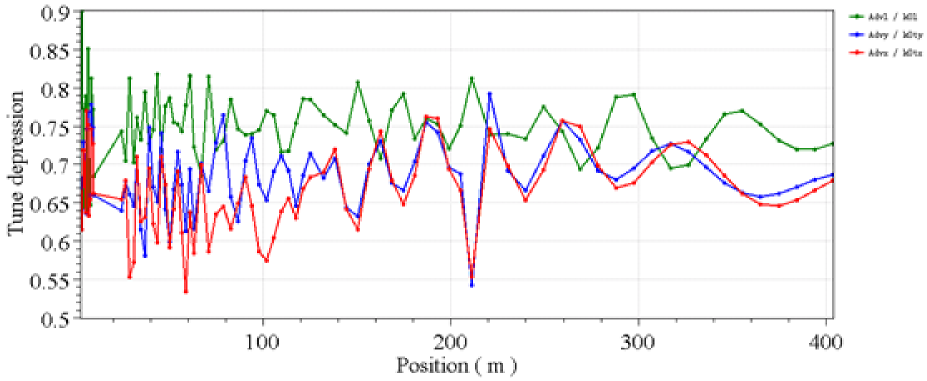

Figure 5: Tune depressions along the CADS linac are larger than 0.5.

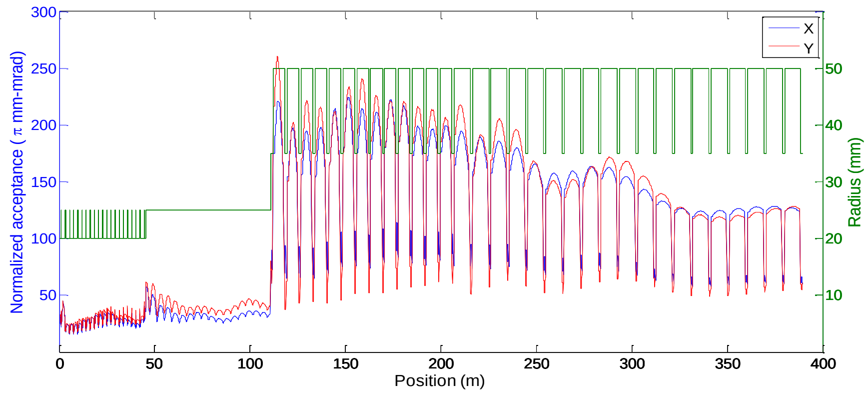

Figure 6: Apertures and transverse acceptance along the main linac.

5) Low enough synchronous phases to get large longitudinal phase acceptance especially in low energy section. The following forma is the longitudinal phase advance.

$$\sigma_{l0} = \sqrt{LP}k_{l0} = \sqrt{-\frac{2\pi E_0 TL\sin(\varphi_s)P}{mc^2(\beta\gamma)^3\lambda}}$$

where φ_s is synchronous phase, E_0TL is effective votlage, β,γ is lorentz factor, λ is wavelength, and P is period length. To get reasonable and optimized design, we should balance phase advanace, accelerating gradient and longitudinal phase acceptance.

6) For the transverse acceptance we adopt the aperture is larger than 10 times rms beam size and the acceptance in crymodules is larger than 2 times the acceptance in warm transitions [9], which is shown in Fig.6.

2.1.2. Baseline design

The CADS accelerator is composed of two parallel injectors, a joint MEBT line, a main linac, and a HEBT line. The injectors is composed of an ion source, a low energy beam transport line (LEBT), a room temperature RFQ (162.5 MHz or 325 MHz), a medium energy beam transport line (MEBT), two cryogenic module of spoke cavities (β=0.12) or HWR cavity (β=0.09) and a medium energy beam transport line (MEBT2) [10]. The main linac have four accelerating section: Spoke021 section (325 MHz), Spoke040 section (325 MHz), Ellip063 (650 MHz) and Ellip082 (650 MHz), which is shown in Fig.7.

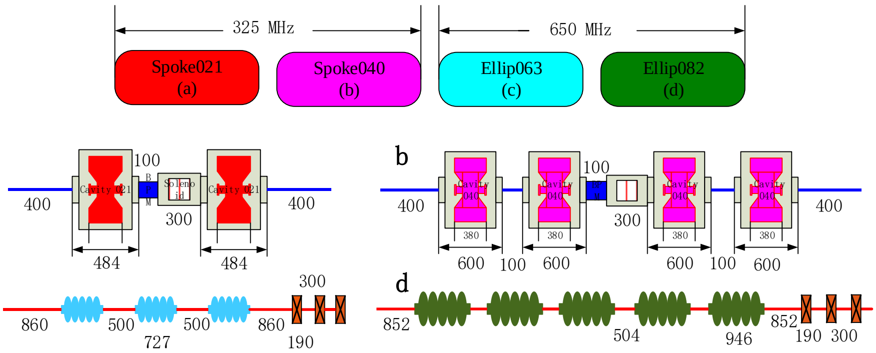

Figure 7: Schematic view of the lattice structures for the main linac sections.

Table 2: Main parameters of the main linac

	RFQ	Spoke012	Spoke021	Spoke040	Ellip063	Ellip082	Total
Energy (MeV)	3.2	10	38	149	399	1504	1504
Cavity no.	1	14	36	60	42	100	252
Focusing		RS	RSR	R^2SR^2	R^3FDF	R^5FDF	
CM no.		2	6	15	14	20	57
Synch. phase		-35~-25	-42~-30	-27~-22	-20~-18	-15~-14	
Section leng.(m)		10.006	39.024	57.84	84.336	191.8	383

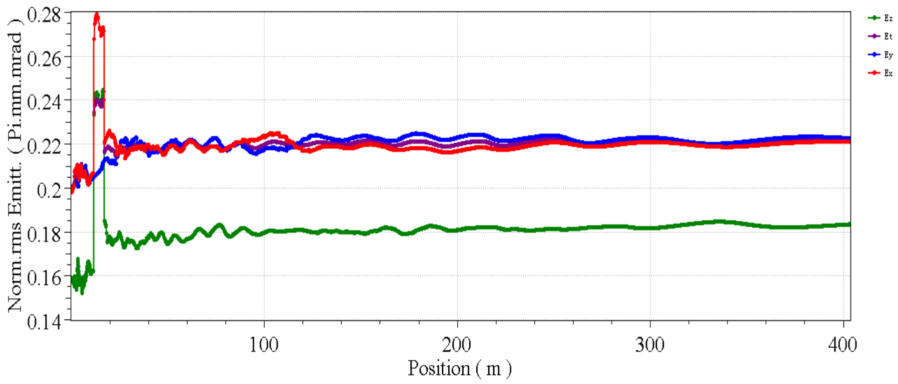

Figure 8: Emittance along the CADS linac.

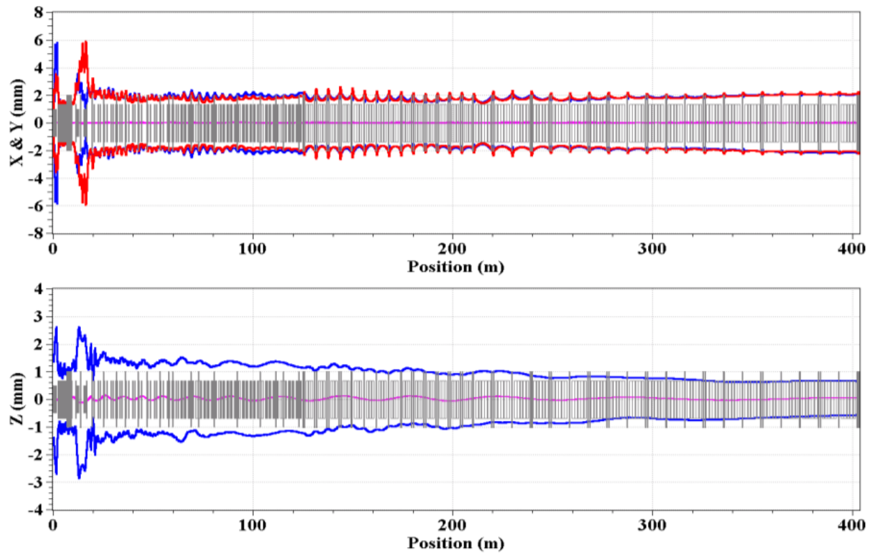

Figure 9: Beam envelope along the CADS linac.

Based on the design rules and error study the baseline design have been presented and main parameters of main linac is shown in Table 2. Figure 8 shows the emittance growth along the CADS linac and Figure 9 shows the beam envelope along the linac. The emittance growth is 12% in transverse plane and 16% in longitudinal plane and beam envelope is very smooth with good matching. From the beam dynamic results one can see the baseline design have very good performance.

2.1.3. Beam loss control

One key point in designing the linac is that beam losses should be kept as low as possible along the linac, with a usual acceptance of 1 W/m for all high-power proton accelerators. So the beam loss prediction and control is the most important issuse after the finished baseline design. For the CADS accelerator, the beam loss acceptance means a beam-loss rate of 7×10^{-8}/m at the higher-energy part. Strippings are very important beam loss mechanism for H^- accelerator. Fortunately the particle is proton for CADS accelerator and avoid one major beam loss mechanism. Another beam loss mechanism is emittance growth caused by non-linear space charge, resonances, anisotropy, instability, initial density profile mismatch and so on and beam halo caused by mismatch. Error study and mismatch study is the most effective method to predict beam loss and optimize baseline design to get larger tolerance.

2.1.3.1. Error study

All the devices having electromagnetic field influence over the beam should have installation errors including translational errors and rotational errors, and also field errors. We can classify the possible error sources into three groups:

1) Misalignment errors: affecting all the elements with translational errors and rotational errors, e.g. solenoids, quadrupoles, accelerating cavities, etc.
2) Field errors: affecting the field levels as well as the phases of RF cavities and the fields of magnets.
3) BPM uncertainty errors: affecting the orbit correction effect.

All the errors can be also classified in two different types according to their variation properties with time: static errors and dynamic errors. In a real machine, the effect of static errors can be partially corrected with the help of beam measurements. After detailed analysis [11] amplitudes of errors are determented shown in Table 3. Error study can examine the performance of lattice design and give guide to optimize lattice design. An improved lattice for injector-I after error study is proven to have better error tolerance[12] and the acceptance are shown in Fig.10.

Table 3：Amplitudes of errors used for error studies

Error No.	Error description	Tolerance	
		Static	Dynamic
1	Magnetic element displacement		
	Quadrupole	0.1 mm	2 µm
	Solenoid (cold)	1 mm	10 µm
2	Magnetic element rotation	2 mrad	0.02 mrad
3	Magnetic element field	0.5 %	0.05%
4	Cavity displacement (cold)	1 mm	10 µm
5	Cavity rotation	2 mrad	0.02 mrad
6	RF amplitude fluctuation	1%	0.5%
7	RF phase fluctuation	1°	0.5°
8	BPM uncertainty	0.1mm	

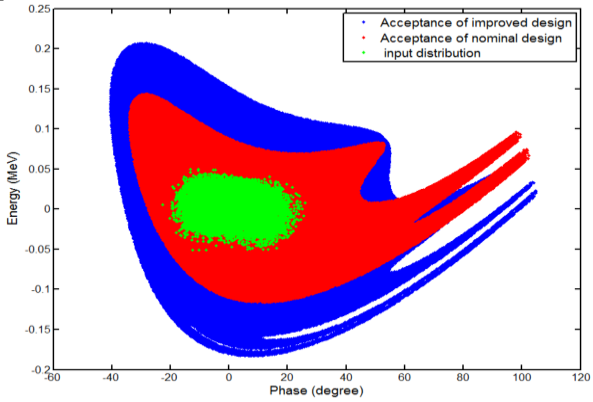

Figure 10: Comparison between the acceptances of the nominal and the improved lattices.

The iterations between lattice design and error study of main linac have been finished two times and one have got the baseline design, however the optimization is still undergoing. The error study of end-to-end have been finished. Figure 11 shows the beam orbit with errors and correction. The results of error study are shown in Fig.12 and Table 4, which are acceptable.

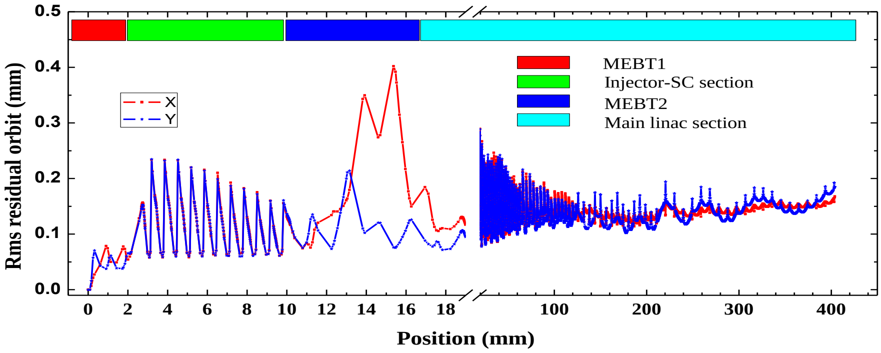

Figure 11: Beam orbit of linac with errors and corrections.

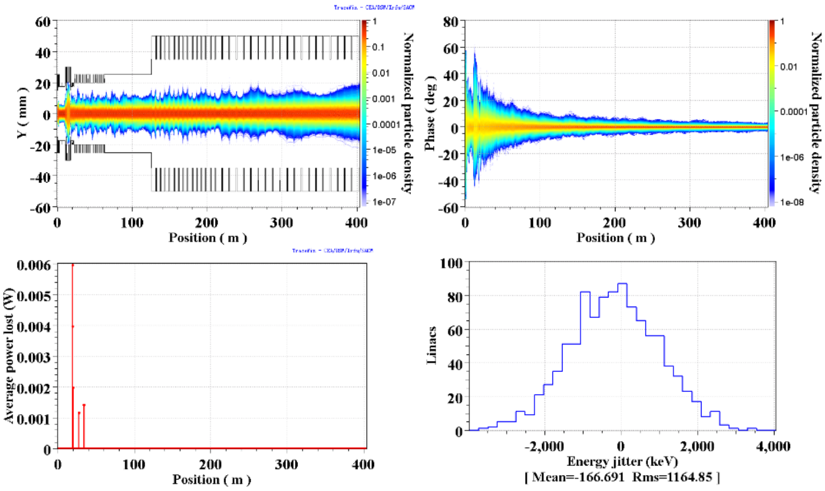

Figure 12: Particle trajectories in horizontal plane (up-left) and in longitudinal plane (up-right), beam loss power (down-left) along the linac and energy jitter (down-right) at exit of linac.

Table 4: Emittance growth, energy jitter and beam loss rate of baseline design with errors

	ε_x (rms)	ε_y (rms)	ε_z (rms)	Energy jitter	Beam loss
Unit		%		keV	
Baseline deisgn	11.8	12.0	15.3	0	0
Baseline deisgn with errors	34.8(11.0)	37.1(12.7)	33.7(11.9)	1165	1.6×10^{-7}

2.1.3.2. Mismatch study

The emittance growth due to mismatch should be carefully considered in the ADS accelerator where the beam loss is concerned. With the presence of nonlinear components, the filamentation effect will lead to a real emittance dilution, and the betatron modulation has a similar impact. More than filamentation, a mismatched beam can be unstable if the channel working point is not properly set. Mismatch study of main linac have been presented [13]. Figure 13 shows the parametric resonance between single particle and envelope oscillation for bunched beam and the results of emittance growth are shown in Table 5. The transverse mismatch factor should be smaller than 0.4 and longitudinal mismatch smaller than 0.3 to meet the emittance growth requirement. Figure 14 shows the envelope oscillation with 0.4 mismatch in the transverse and 0.3 mismatch in the longitudinal direction, with the envelope oscillation corresponding to the prediction.

Table 5: Emittance growth caused by mismatch

Mode	mismatch factor	Mismatch factor			ε_x	ε_y	ε_z
		x	y	z	%	%	%
Matched	0	0	0	0	2.7	3.2	4.2
Quad.	0.3	+0.3	+0.43	0	23.9	23.3	6.9
High	0.3	+0.08	+0.08	+0.3	7.7	9.0	21.2
Low	0.2	-0.4	-0.4	+0.2	28.5	30.0	15.1

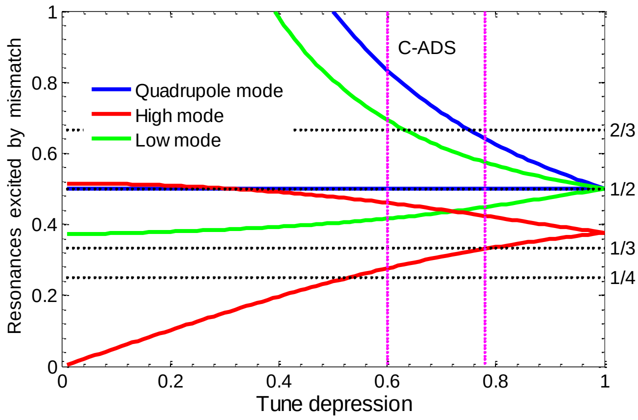

Figure 13: Parametric resonances excited by mismatch.

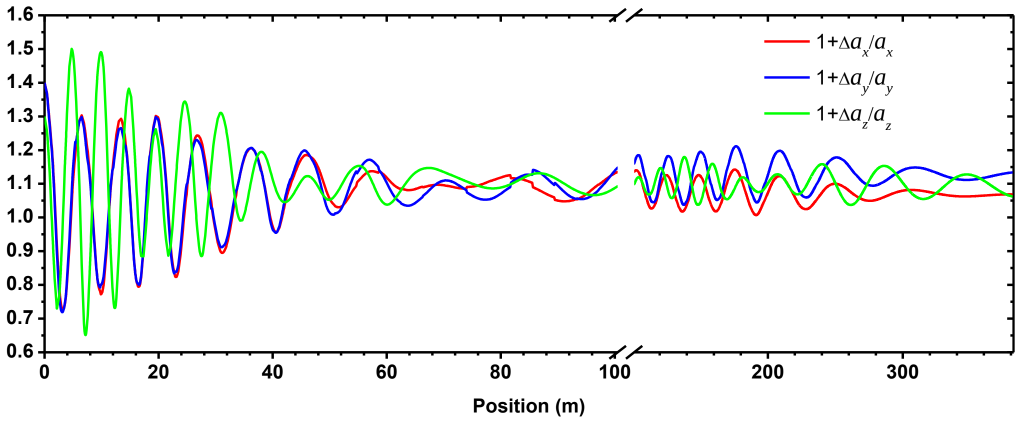

Figure 14: Envelope oscillation with 0.4 mismatch in transverse direction and 0.3 mismatch in longitudinal direction.

3. Redundancy and fault-tolerance study

3.1.1. Introduction

To meet extremely high reliability and availablity requirement it is very important to have fault-tolerant capablities in the physics design besides all the hardware will be operated with good performance and redundancy. For the injector we adopt " Hot-standby" or parallel method and for the main linac we can adopt global or local compensation-rematch method. When one element is failure, the global compensation-rematch method is retuning and rephrasing of all elements after the failure element to reconver energy and rematch the focuing to the linac exit. The global compensation-rematch method is retuning and rephrasing of all following elements and take a few minutes [14], however this mehtod can save a lot of cost for power source for a litter redundancy. The local compensation-rematch method is retuning and rephrasing of neighbouring elements to reconver the nominal energy and phase and rematch the focuing to the matching point where is the following neighbouing point of failure element, which is shown in Fig.15. This method is only retuning and rephrasing of neighbouring elements and independence and locality. In this way, more cavity failures in different locations at the same time can be compensated independently and efficiently, which is also an important aspect in ADS applications. In addition, the failures of focusing elements can be also re-matched locally. To achieve this goal, the design has made 30% redundancy in the nominal field level to all the cavities, which means about 70% power supply margin [15]. So the cost is the most problem for local compensation-rematch method.

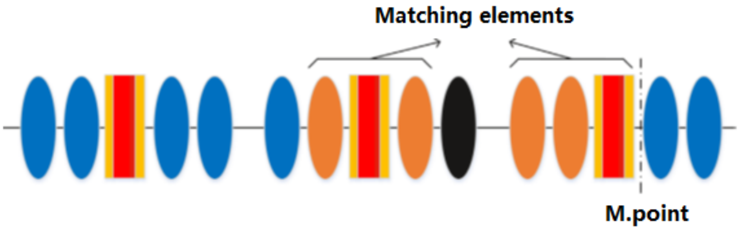

Figure 15: Local compensation–rematch for a cavity failure. The blue ellipses stand for normal cavities, the rectangular shape for foucing elements, the black ellipse for the failed cavity, and the orange ellipses for compensation-rematch cavities, M.point stands for the matching point. The compensation-rematch cavities are retuned to reconver the nominal beam energy, phase and twiss paramenters at the point M.

3.1.2. Local compenstation-rematch method for CADS main linac [16]

In the Ref.[16] detailed analysis of local compenstation-rematch method with failures of caivth and foucing elements in different sections have been presented. The method is success fully applied in the CADS main linac. It is very effective in keeping the good beam quality in the case of failures of both RF cavity and focusing element. Figure 16 shows beam envelope and emittance growth using local compensation-rematch method with several caivty failures in different section, which is acceptable for the CADS linac design. With more further study one can get that the fault recovery scheme is a feasible everywhere in the CADS main linac to compensation-rematch for the loss of a single cavity or even of two neighbouring cavities in high energy section.

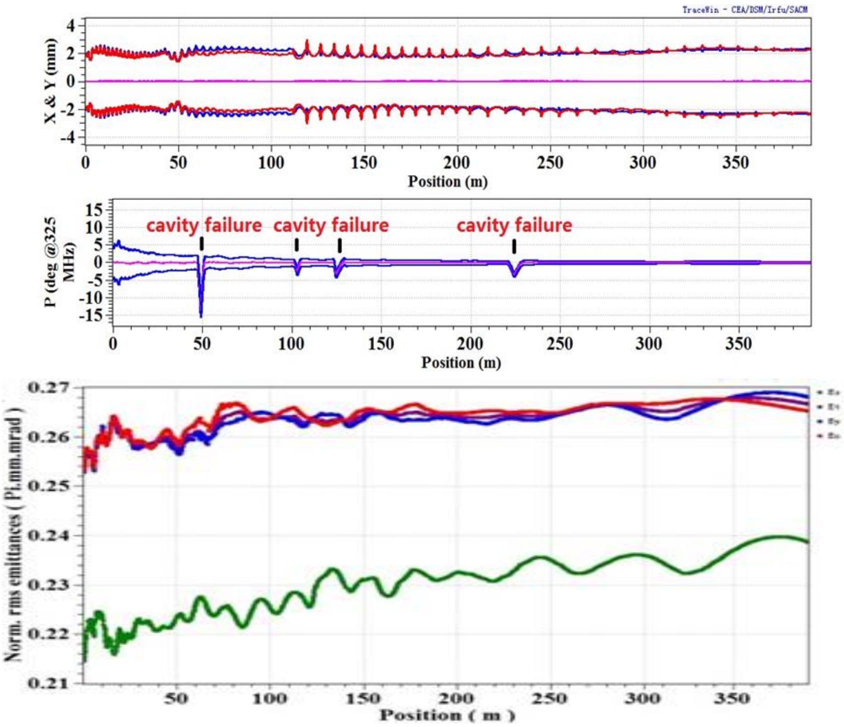

Figure 16: Beam envelope (up) and emittance growth (bottom) in both the transverse and longitudinal planes using local compensation-rematch method with several caivty failures in different section.

3.1.3. Realization of "Hot-standby" for injector

To realize the "Hot-standby" within very short time *t* there are 4 steps shown in Fig.17.

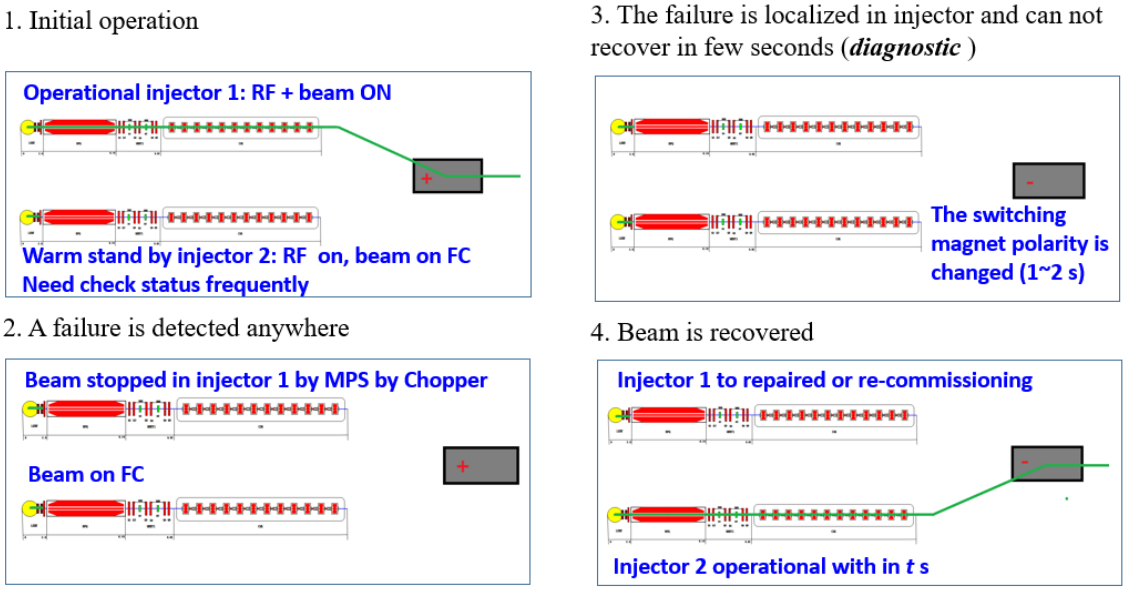

Figure 17: Realization of "Hot-standby" method for injecots.

3.1.4. Realization of local compensation-rematch method

Figure 18 shows the logic diagram of realization of local compensation-rematch method. Specially mentioned we need very good and rigorous diagnostic system. Now the tuning speed of tuning system is not fast enough to meet the time requirement and maybe we need cold tuning system.

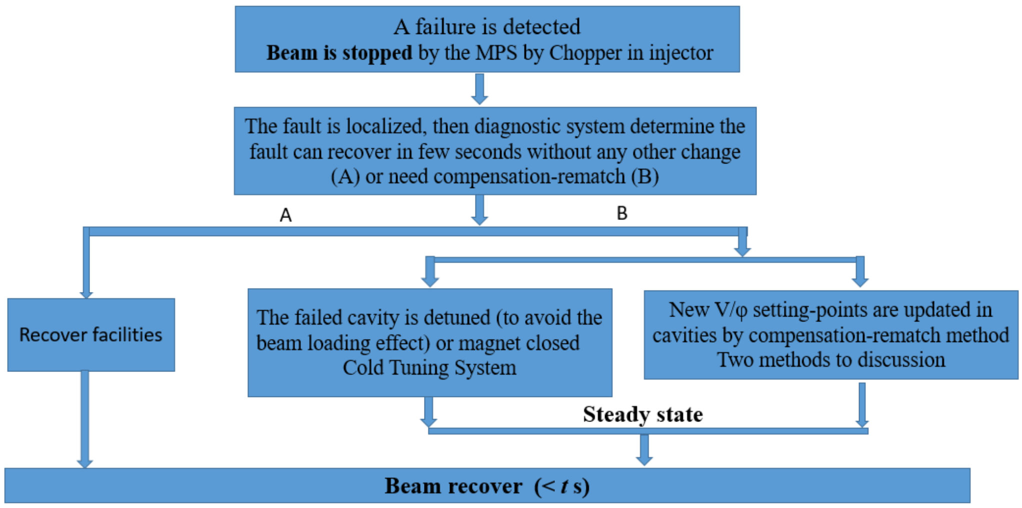

Figure 18:Logic diagram of realization of local compensation-rematch method.

In the openation of accelerator there are two methods to get the new V/φ or magnet setting points with one element failure.

1) Table lookup method: The setting parameters are determined in advance for any element failure and established the database to save all the case. Once the failed index signal is detected, then look up the right setting points. This method is simple and stabilization

and controllable, but need a lot of works in advance for simulation and database establishment (should avoid human error) and the speed should be optimized.

2) Hardware compensation and rematch method [17]: This method is one online method to get the setting parameters using FPGA and optimized algorithm. Arithmetic computing speed of this method is higher, as an integrated circuit device consisting of logic gates, an FPGA is able to realize parallel calculating and synchronous processing. Instantaneous compensation and rematch using this method is easier, because it's an easier way to connect with the low level RF system and other types of hardware facilities. This method have very good portability and repeatability and no need a lot of calculation in advance. However, between models in FPGA and dynamic simulation have errors and this method is not very controllable, which need more consideration and judge on the results.

4. Beam commissioning of CADS injector-I

To authentication the technology road one test stand with 10 MeV have been installed, which is composed of an ECT ion source, a LEBT, a RFQ, an MEBT1, two cryogenic module with 14 cavities, 14 solenoids and 14 cold BPMs and a beam dump line. Until July 2016 we have commissioned the 10.67 MeV and 10.6 mA beam.

4.1.1. RFQ commissioning

The layout of the RFQ commissioning test stand is shown in Fig.19 and beam commissioning have been finished [18]. With the repetition frequency 50 Hz and pulse length 300 us, we have measured the beam transmission efficiency with different input power, which is shown in Fig.20. We also finished some beam test with high duty factor. At 90% duty factor, we got 11 mA 31 kW proton beam at RFQ exit with 90% beam transmission efficiency, while 95% beam transmission efficiency at 70% duty factor. Figure 21 shows the measured emittance at RFQ exit by double-slits method.

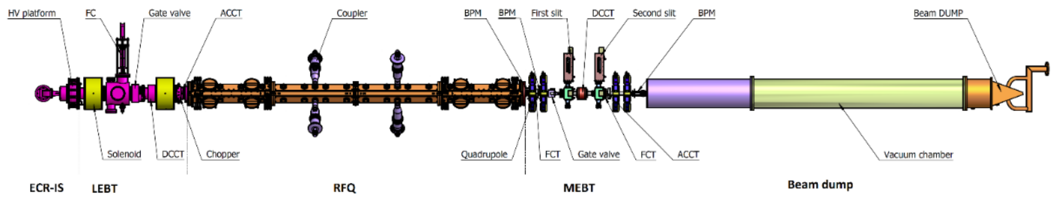

Figure 19: Layout of the test stand for RFQ commissioning.

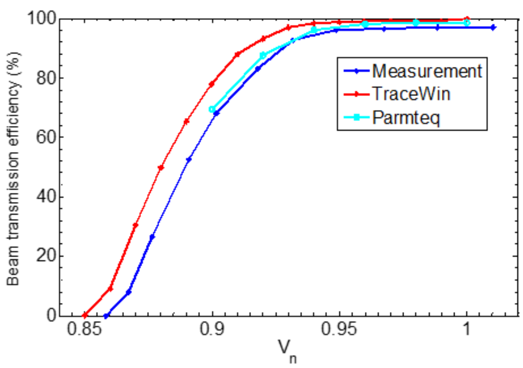

Figure 20: Measured and simulated transmissions of RFQ as functions of the inter-vane voltage Vn.

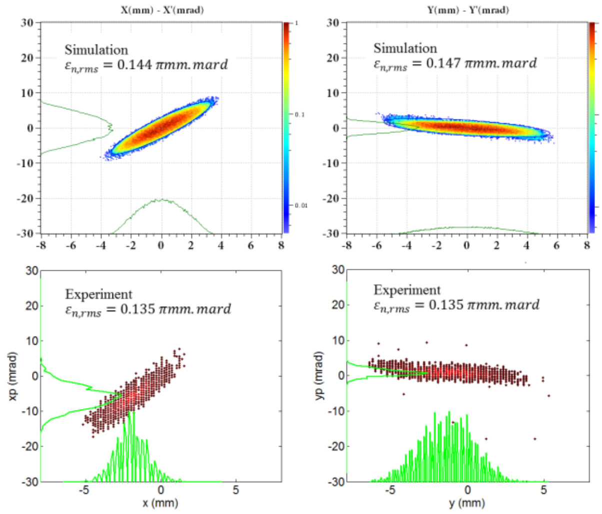

Figure 21: Simulated (up) and measured (down) transverse emittances and beam distribution of the RFQ.

4.1.2. CM1 commissioning

After the beam commissioning of RFQ accelerator and Test Cryogenic Module (TCM) for injector-I, we have finished the beam commissioning of CM1 (Cryogenic Module 1) test stand shown in Fig. 22, which is composed of an ion source, a LEBT, a 325MHz RFQ, a MEBT1, a cryogenic module (CM1) of seven SC spoke cavities (β=0.12), seven SC solenoids, seven cold BPMs and a beam dump line[19]. The beam energy is 6.0 MeV and beam current is 10.6 mA with he repetition frequency 2 Hz and pulse length 1 ms, which is shown in Fig. 23.

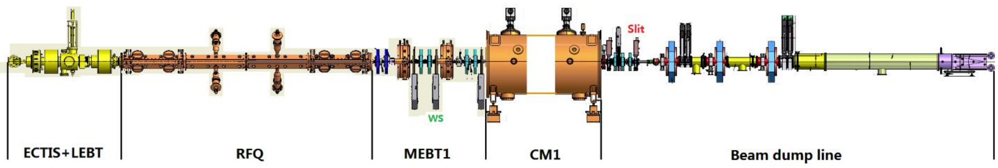

Figure 22: Layout of the CM1 test stand.

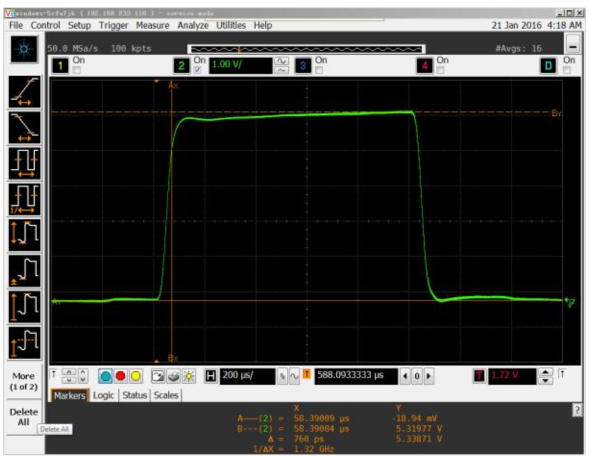

Figure 23: Beam current measurement at CM1 exit by DCCT. The singnal factor is 2 mA/V.

4.1.3. CM2 commissioning

Figure 24 shows the layout of CM2 test stand, which is composed of an ion source, a LEBT, a 325MHz RFQ, a MEBT1, two cryogenic module (CM1 & CM2) of 14 SC spoke cavities (β=0.12), 14 SC solenoids, 14 cold BPMs and a beam dump line. We have finisehd the commissioning of CM2 and the beam energy is 10.67 MeV and beam current is 10.6 mA with he repetition frequency 2 Hz and pulse length 20 μs. The measured energy result with TOF method by two BPMs is shown in Fig. 25 and the measured current result by ACCT is shown in Fig. 26. We also measured the energy spread along pulse length by energy spread analysis system which is 0.32% shown in Fig. 27.

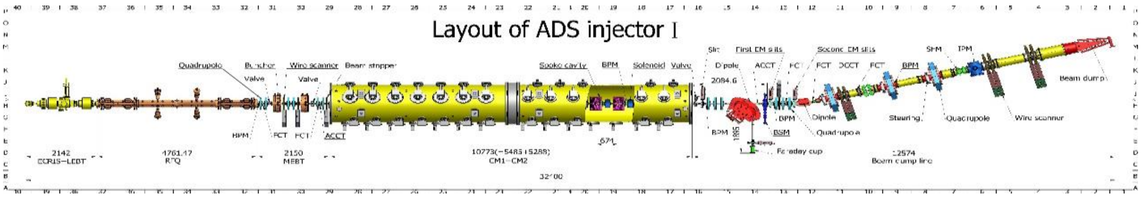

Figure 24: Layout of CM2 test stand.

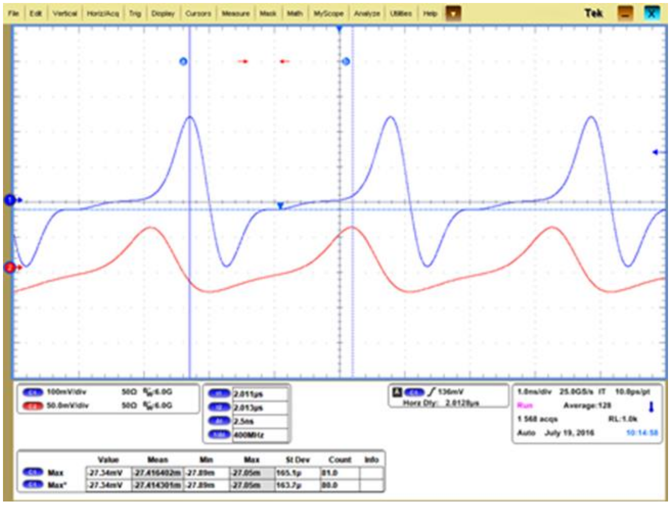

Figure 25: Energy measurment by TOF with BPM.

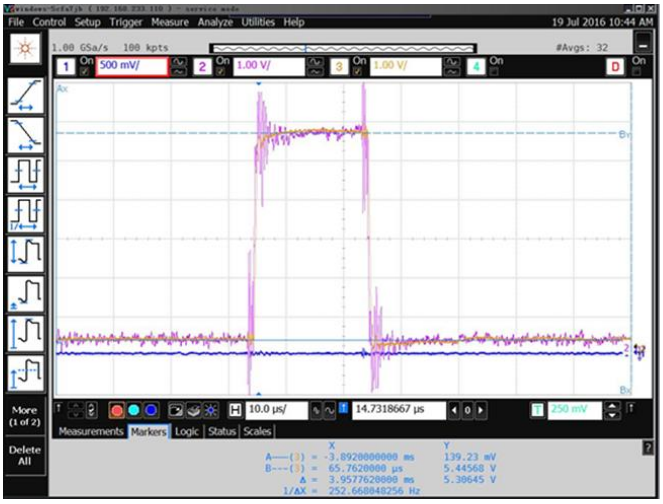

Figure 26: Beam current measurement at CM2 exit by ACCT. The singnal factor is 2 mA/V.

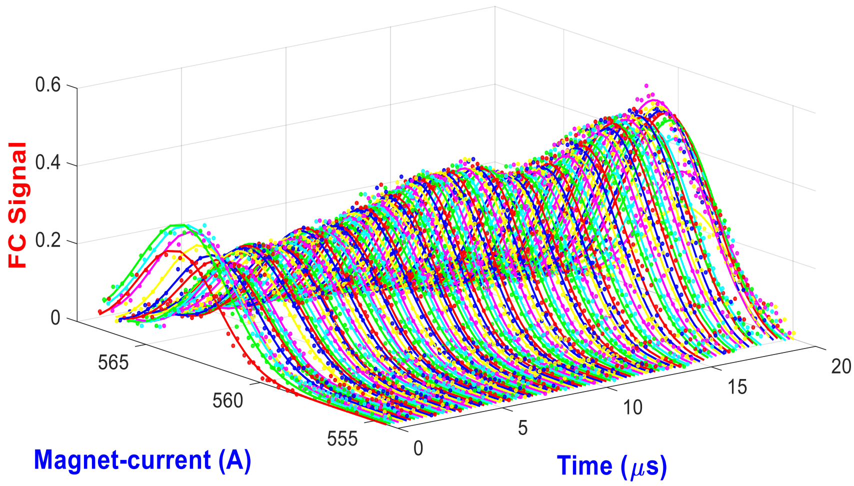

Figure 27: Energy spread measurment by energy spread analysis system.

5. CONCLUSION

To meet the extremely high reliability and availability for high power accelerator, it is very important and imperative to perform robust design and redundancy for element failures. In this paper the robust design including error study and mismatch study and redundancy and fault-tolerance study for the CADS linac have been dicussed. The beam commissioning of CADS injector-I have got 10.67 MeV and 10.6 mA beam.

ACKNOWLEDGMENT

The authors would like to thank all members of C-ADS accelerator team for the accelerator conditioning and commissioning and valuable suggestions and comments.

References

[1] Zhihui Li, et al., *Physics design of an accelerator for an accelerator-driven subcritical system*, PHYSICAL REVIEW ACCELERATORS AND BEAMS, 16, 080101 (2013).

[2] Yuan He, *The present status and future plans of Chinese ADS project*, in Proceedings of *4th Workshop on ADS and thorium*, University of Huddersfield, England, 2016.

[3] R. L. Sheffield, *Utilization of Accelerators for Transmutation and Energy Production*, in Proceedings of *HB2010*, Morschach, Switzerland, 2010.

[4] Martin Reiser, *Theory and design of charged particle beams*, JOHN WILEY & SONS, INC, 1994.

[5] Ingo Hofmann, *Incoherent and coherent resonant space charge phenomena*, report of *Space charge workshop 2015*, Oxford, March, 2015.

[6] I. Hofmann, *Stability of anisotropic beams with space charge*, PHYSICAL REVIEW E, Vol.57, No.4, 1998.

[7] C. Meng, et al., *Designs of high-intensity proton linacs with non-equipartitioning*, in Proceedings of *IPAC2014*, Dresden, Germany, 2014.

[8] J-M. LAGNIEL, *Halos and chaos in space-charge dominated beams*, in Proceedings of *EPAC96*, Barcelona, Spain, 1996.

[9] C. Meng, Z. H. Li, J. Y. Tang, F. Yan, *Error analysis and beam loss control in the c-ads main linac*, in Proceedings of *IPAC2013*, Shanghai, China, 2013.

[10] Fang Yan, et al., *Physics design of a 10 MeV injector test stand for an accelerator-driven subcritical system*, PHYSICAL REVIEW ACCELERATORS AND BEAMS, 18, 054201 (2015).

[11] C. Meng, *Error analysis and beam loss mechanism of the C-ADS linac*, Ph.D. theses, China, 2014.

[12] C. Meng, Z. H. Li, J. Y. Tang, *Error analysis and lattice improvement for the C-ADS Injector-I*, Chinese Physics C, Vol. 38, No. 6 (2014) 067008.

[13] C. Meng, J. Y. Tang, S. L. Pei, F. Yan, *Mismatch study of C-ADS main linac*, Chinese Physics C, Vol. 39, No. 9 (2015) 097002.

[14] Sang-ho Kim, *SNS superconducting linac operational experience and upgrade path*, in Proceedings of *LINAC08*, Victoria, Canada, 2008.

[15] F.Bouly, et al., *Preliminary study of constraints, risks and failure scenarios for the high luminosity insertions at HL-LHC*, in Proceedings of *IPAC2014*, Dresden, Germany, 2014.

[16] Biao Sun, et al. *Local compensation–rematch for major element failures in superconducting linacs with very high reliability and low beam loss*, Nuclear Instruments and Methods in Physics Research A 785 (2015) 77–86.

[17] Z. Xue, J. P. Dai, C. Meng, *A new method for compensation and rematch of cavity failure in the C-ADS linac*, Chinese Physics C, Vol. 40, No. 6, (2016) 067003.

[18] C. Meng, et al., *Beam commissioning of C-ADS injector-I RFQ accelerator,* in Proceedings of IPAC2015, Richmond, USA, 2015.

[19] Fang Yan, Huiping Geng, Cai Meng, Yaliang Zhao, *Commissioning of the China-ADS injector-I testing facility,* in Proceedings of *IPAC2016*, Busan, Korea, 2016.